

## OPTIMIZATION OF MULTILAYER ACTIVE MAGNETIC REGENERATORS

**Jean Cararo, jean.cararo@polo.ufsc.br**

**Jaime Lozano, jaime@polo.ufsc.br**

**Jader Barbosa Jr., jrb@polo.ufsc.br**

POLO — Research Laboratories for Emerging Technologies in Cooling and Thermophysics, Department of Mechanical Engineering, Federal University of Santa Catarina, Florianópolis, SC, 88040-900, Brazil.

**Paulo Trevizoli, paulot@uvic.ca**

**Reed Teyber, rteyber@uvic.ca**

**Andrew Rowe, arowe@uvic.ca**

IESVic — Institute for Integrated Energy Systems, Department of Mechanical Engineering, University of Victoria, 3800 Finnerty Rd, Victoria, B.C. V8W 3P6, Canada.

**Abstract.** *Magnetic refrigeration harvests the magnetocaloric effect (MCE) in regenerative thermodynamic cycles by means of magnetic work on an active magnetic regenerator (AMR). Since the MCE of typical materials is large only over a narrow temperature range, layered regenerators can improve the AMR temperature span and thermal performance by using materials with different transition (Curie) temperatures ( $T_C$ ) to enhance the MCE along the regenerator bed. In this work, a numerical model is used to simulate layered AMRs. Experimental magnetocaloric properties of Gd spheres are employed to simulate three different  $Gd_{1-x}Y_x$  alloys with  $T_C = 277$  K ( $x = 0.075$ ),  $T_C = 283$  K ( $x = 0.05$ ),  $T_C = 286$  K ( $x = 0.025$ ) and  $T_C = 290$  K ( $x = 0$ ). Layered AMRs with two to four layers have been studied by varying the layer length proportions and the  $Gd_{1-x}Y_x$  alloy type. Two different temperature spans of 15 and 20 K were considered. Optimized layered AMRs are found when a given proportional layer length combination returns the highest cooling capacity for a fixed temperature span. To perform a more meaningful optimization analysis, heat leaks or gain are included in the simulations. It was observed that the cooling capacity increases with the number of layers, where a maximum 49.6% increase in the cooling capacity was achieved by a four-layer regenerator in comparison with a single-layer regenerator, for a temperature span of 20 K.*

**Keywords:** *Magnetic refrigeration; magnetocaloric effect; active magnetic regenerator; multilayer.*

### 1. NOMENCLATURE

<i>Roman</i>		$u$	Superficial (Darcy) velocity [m/s]
$c$	Specific heat capacity [J/kg K]	$z$	Axial coordinate [m]
$c_p$	Specific heat capacity at constant pressure [J/kg K]	<i>Greek</i>	
$c_E$	Ergun constant [-]	$\beta$	Surface area density [m <sup>2</sup> /m <sup>3</sup> ]
$D$	Diameter [mm]	$\Delta T_{ad}$	Adiabatic temperature change [K]
$D_{  }$	Longitudinal thermal dispersion [m <sup>2</sup> /s]	$\Delta T_{sys}$	System temperature span [K]
$h$	Convective heat transfer coefficient [W/m <sup>2</sup> K]	$\varepsilon$	Porosity [-]
$H$	Magnetic field [T]	$\mu$	Dynamic viscosity [Pa s]
$k$	Thermal conductivity [W/m K]	$\rho$	Density [kg/m <sup>3</sup> ]
$K$	Permeability of the porous medium [m <sup>2</sup> ]	<i>Subscripts and superscripts</i>	
$L$	Length [mm]	$eff$	Effective
$p$	Pressure [kPa]	$f$	Fluid phase
$\dot{q}_{csg}$	Casing heat transfer [W/m <sup>3</sup> ]	$s$	Solid phase
$\dot{Q}_C$	Cooling capacity [W]		
$T$	Temperature [K]		
$t$	Time [s]		

## 2. INTRODUCTION

The magnetocaloric effect (MCE) is a thermodynamically reversible phenomenon observed in certain magnetic materials that are susceptible to a temperature change when subjected to an external magnetic field. The EMC can be used to build an internally-reversible thermodynamic cycle (i.e., Brayton, Stirling, Ericsson), which is called magnetic refrigeration.

After the cyclic steady state operation is achieved in an active magnetic regenerator (AMR), a temperature profile is established along the magnetocaloric material (MCE) between the hot and cold sources. Since the MCE of a magnetocaloric material is larger around its Curie temperature ( $T_C$ ), regenerators with layers of materials with different  $T_C$  may improve the AMR temperature span due to an effective use of the MCE along the porous bed.

The performance of multilayer AMRs has been studied numerically and experimentally. Nielsen *et al.* (2010) modified a two-dimensional numerical model to investigate two-layer parallel-plate AMRs. The analysis was carried out by varying  $T_C$  and the fraction of the regenerator occupied by each layer. Gadolinium (Gd) was assumed as the magnetocaloric material (MCM), and the MCE was modeled through the mean field model (MFM). By grading different materials in the regenerator, higher cooling capacities and larger temperature spans were attained when compared with a single-layer AMR. You *et al.* (2016) employed a one-dimensional AMR model to study the performance of a two-layer regenerator composed of Gd and  $Gd_{0.73}Tb_{0.27}$  for different system temperature spans ( $\Delta T_{sys}$ ). They concluded that the two-layer AMR can effectively improve the cooling capacity ( $\dot{Q}_C$ ) and the coefficient of performance (COP) at larger  $\Delta T_{sys}$ . A numerical evaluation of the performance of multilayer parallel-plate and microchannel regenerators was carried out by Kamran *et al.* (2016) employing compounds of  $LaFe_{13-x}yCo_xSi_y$  and hypothetical compounds of Gd. They reported that when the number of layers is increased, the cooling capacity is also increased for a certain  $\Delta T_{sys}$ , and for a given length of the regenerator there is an optimum number of layers that yield the maximum performance.

The performance of a two-layer regenerator composed of Gd and three different  $Gd_{1-x}Y_x$  alloys was evaluated numerically and experimentally by Teyber *et al.* (2016). The results were compared with those of a single-layer Gd regenerator. The experiments were performed in the AMR test apparatus (PM II) developed by Arnold *et al.* (2014). The authors reported higher maximum temperature spans for the two-layer regenerator. Jacobs *et al.* (2014) designed and constructed a large-scale magnetic refrigeration system using six layers of  $LaFeSiH$  of different Curie temperatures. This system attained an impressive cooling capacity of about 3 kW at zero temperature span. Eriksen *et al.* (2015) built a rotary AMR using 11 regenerator beds composed of spheres of Gd and three  $Gd_{1-x}Y_x$  compounds. They achieved the best values reported in the open literature for the coefficient of performance (COP) for ranges of cooling capacities compatible with a domestic refrigerator.

In the present work, a one-dimensional AMR numerical model developed by Trevizoli (2015) has been modified to evaluate multilayer packed-bed regenerators. Experimental magnetocaloric properties of Gd have been employed to simulate three other  $Gd_{1-x}Y_x$  alloys. AMRs with two, three and four layers with different layer lengths have been optimized in terms of the maximum cooling capacity for a given  $\Delta T_{sys}$ .

## 3. METHODOLOGY

### 3.1 Mathematical modeling

The AMR numerical model developed by Trevizoli (2015) is composed of the one-dimensional Brinkman-Forchheimer equation, which describes the flow in the porous media coupled with energy balance equations for the solid and fluid phases. The assumptions are one-dimensional, laminar and incompressible fluid flow, low porosity ( $\varepsilon < 0.6$ ) and absence of body forces. Thus, the momentum equation is given by:

$$\frac{\rho_f}{\varepsilon} \left( \frac{\partial u}{\partial t} \right) = - \frac{\partial p}{\partial z} - \frac{\mu_f}{K} u - \frac{c_E \rho_F}{K^{1/2}} |u| u \quad (1)$$

where  $\rho_f$  and  $\mu_f$  are the fluid density and the fluid kinematic viscosity, respectively,  $\varepsilon$  is the porosity,  $K$  is the permeability of the porous medium,  $u$  is the Darcian velocity,  $t$  is the time,  $p$  is the pressure,  $z$  is the axial distance and  $c_E$  is the Ergun constant. The terms on the right side of Eq. (1) are the term of the pressure gradient, Darcy term viscous flow through porous media and the Forchheimer term (inertial effects), respectively.

In addition to the momentum equation, it is necessary to solve the energy balance equations for the solid and the fluid. The energy equation for the fluid flow, considering the assumptions of one-dimensional, laminar and incompressible fluid flow, is given by:

$$\rho_f c_{p,f} \left( \varepsilon \frac{\partial T_f}{\partial t} + u \frac{\partial T_f}{\partial z} \right) = -h\beta(T_f - T_s) + \varepsilon(k_f^{eff} + \rho_f c_{p,f} D_{||}) \frac{\partial^2 T_f}{\partial z^2} + \left| u \frac{\partial p}{\partial z} \right| + \dot{q}_{csg} \quad (2)$$

where  $T_f$  is the fluid temperature and  $T_s$  is the solid temperature,  $h$  is the interstitial convective heat transfer coefficient,  $\beta$  is the surface area density,  $k_f^{eff}$  is the effective thermal conductivity of the fluid phase,  $c_{p,f}$  is the fluid specific heat capacity,  $D_{||}$  is the longitudinal thermal dispersion and  $\dot{q}_{csg}$  is the casing heat transfer loss. The terms on the left side of Eq. (1) are due to inertial effects (thermal capacity) and longitudinal advection. The terms on the right side are the heat transfer calculated using a convective heat transfer coefficient, axial conduction and viscous dissipation.

The energy equation for the solid phase is given by:

$$\rho_s c_s (1 - \varepsilon) \frac{\partial T_s}{\partial t} = h\beta(T_s - T_f) + (1 - \varepsilon)k_s^{eff} \frac{\partial^2 T_s}{\partial z^2} \quad (3)$$

where  $\rho_s$ ,  $k_s^{eff}$  and  $c_s$  are the density, the effective thermal conductivity and the specific heat capacity of the solid phase, respectively. The term on the left side of the Eq. (3) represents the thermal inertia in the solid, and the terms on the right side are the interstitial heat convection and axial heat conduction, respectively. The MCE is implemented using the so-called discrete approach, therefore a source term isn't included in Eq. (3). The discrete approach consists of a direct temperature increment or reduction (magnetization or demagnetization), and is given by:

$$T_s(t + \Delta t, z) = T_s(t, z) + \Delta T_{ad}(\Delta H, T_s(t, z)) \quad (4)$$

where  $\Delta H$  is the magnetic field change. Further details about the mathematical model can be found in Trevizoli (2015).

In this work, the AMR numerical model developed by Trevizoli (2015) was adapted to allow the evaluation of multilayer regenerators with up to five layers of MCM with different lengths proportions and different Curie temperatures. Since the model is based on the finite volume method (FVM), the regenerator length is divided into a given number of volumes. Figure 1 shows a representation of a four-layered AMR, where  $L_1$ ,  $L_2$ ,  $L_3$  and  $L_4$  are the length of each layer in the regenerator,  $D$  and  $L$  are diameter and the length of the regenerator, respectively, and  $X_i$  represents a boundary volume. When the volume contains only one kind of MCM, the properties (entropy, specific heat capacity and magnetization) of this volume are the properties of that material. However, when the volume contains a boundary between two layers of MCM (represented by  $X_i$  in Fig. 1), the properties of the volume are given by the mass weighted average of the properties of each MCM inside the volume.

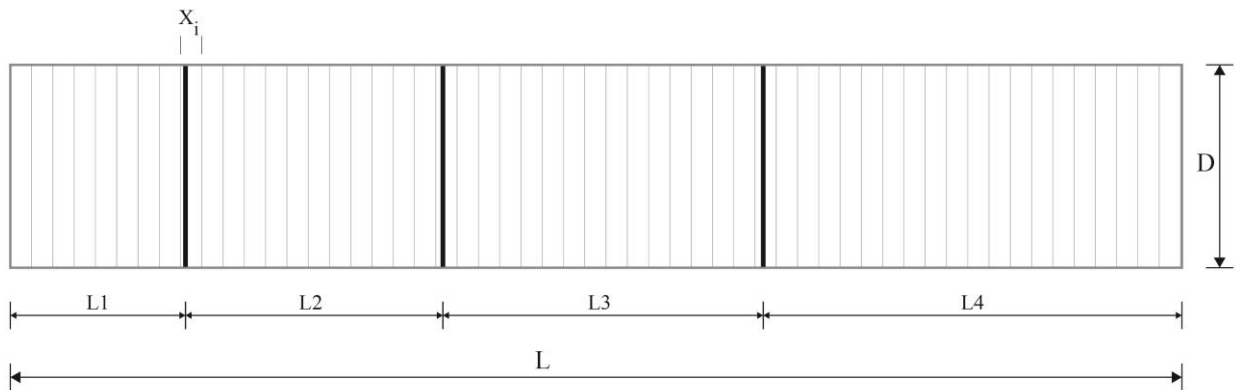


Figure 1. Numerical mesh representation for a four-layered AMR.

### 3.2 Simulation parameters

The MCM properties are based on experimentally determined properties of Gd (with  $T_C = 290$  K). The  $Gd_{1-x}Y_x$  alloys (Teyber *et al.*, 2016) are assumed to have thermophysical properties identical to Gd, except for  $T_C$ , which is shifted to lower temperatures according to the stoichiometry of the alloy. In this work, in addition to Gd, the following alloys were considered:  $Gd_{0.975}Y_{0.025}$  with  $T_C = 286$  K,  $Gd_{0.95}Y_{0.05}$  with  $T_C = 283$  K and  $Gd_{0.925}Y_{0.075}$  with  $T_C = 277$  K. The search for the best AMR configuration was carried out by varying the length of each MCM layer in the regenerator and evaluating its performance in terms of the cooling capacity ( $\dot{Q}_C$ ) for a fixed system temperature spans ( $\Delta T_{sys}$ ).

The numerical simulations were performed based on the operating conditions of the Permanent Magnet Magnetic Refrigerator (PMMR II) experimental apparatus developed by Arnold *et al.* (2014). The operating AMR frequency was

0.5 Hz and the average mass flow rate was 52 kg/h (sinusoidal flow profile). This corresponds to a constant utilization factor of about 0.60. The hot reservoir temperature was maintained at 298 K while two different cold reservoir temperatures were simulated, 283 and 278 K, resulting in two  $\Delta T_{sys}$  of 15 and 20 K, respectively. The packed-bed regenerator was assumed to be composed of spheres with an average diameter of 450  $\mu\text{m}$  and a porosity of 0.36. The bed dimensions were 130 mm (length), 22.4 mm (internal diameter) and 0.9 mm (casing thickness). The heat transfer fluid was a mixture of water and ethylene glycol (70/30 %vv.). The magnetic field profile was a rectified cosine function, with an intensity increasing from 0.06 T to a peak field strength of 1.45 T. To perform a more meaningful optimization analysis, heat transfer through the casing (considering an ambient temperature of 293 K) and demagnetization losses were considered in the simulations. Table 1 shows the simulation parameters, such as regenerator geometry, operating conditions and the considered losses.

Table 1 - Simulation Parameters

Regenerator type	AMR
Regenerator geometry	Packed-bed
Magnetocaloric material	Gadolinium (Gd), $\text{Gd}_{1-x}\text{Y}_x$ alloys
Magnetic field Profile	Cosine CCH
Magnetic field (Min./Max.)	0.06 T / 1.45 T
Heat Transfer fluid	Water and Ethylene Glycol Mixture
Ethylene glycol concentration	30%
Pumping Profile	Senoidal
Average Mass flow rate per blow	52 kg/h
Operation frequency	0.5 Hz
Environment temperature	293 K
Temperature span	15 and 20 K
Hot reservoir temperature	298 K
Cold blow/hot blow time ratio	50%
AMR tubes diameter	22.4 mm
AMR tubes length	130 mm
Average Sphere diameter	450 $\mu\text{m}$
Porosity of AMR matrix	0.36
Losses	Demagnetization, casing heat transfer

#### 4. RESULTS

Initially, simulations of single-layer regenerators considering each MCM were carried out. For a system temperature span of 15 K, a maximum cooling capacity of 24.7 W was attained for  $\text{Gd}_{0.975}\text{Y}_{0.025}$  ( $T_C = 286$  K). For a span of 20 K, a maximum cooling capacity of 13.1 W was achieved using  $\text{Gd}_{0.95}\text{Y}_{0.05}$  ( $T_C = 283$  K).

For the two-layer AMR simulations, Gd was used as the first layer at the hot end of the regenerator, while the other layer (at the cold end) was a  $\text{Gd}_{1-x}\text{Y}_x$  alloy. The fraction of each MCM was varied in steps of 5% of the total length of the regenerator. Since the regenerator composed of Gd and  $\text{Gd}_{0.975}\text{Y}_{0.025}$  presented lower performance than the other  $\text{Gd}_{1-x}\text{Y}_x$  alloys, only the cooling capacity as a function of the fraction of  $\text{Gd}_{0.925}\text{Y}_{0.075}$  and  $\text{Gd}_{0.95}\text{Y}_{0.05}$  in the regenerator length are shown in Figs. 2(a) and 2(b), respectively. The performance was evaluated for  $\Delta T_{sys}$  of 15 and 20 K. The numerical results for two-layer regenerators in Fig. 2 have been compared and validated with the experimental results obtained by Teyber *et al.* (2016) for cases with 50% of Gd for both combinations. Here, it is worth to point out that the extreme values of 0 and 100% in Fig. 1 represent the cooling capacity of a single layer regenerator of each MCM at the given  $\Delta T_{sys}$ . The maximum cooling capacity for a temperature span of 15 K (27.3 W) was attained by a regenerator composed of 40% of  $\text{Gd}_{0.95}\text{Y}_{0.05}$  and 60% of Gd. This corresponds to a 10.5% performance increase compared to a single-layer regenerator. On the other hand, the maximum cooling capacity for a temperature span of 20 K (16.7 W) was achieved with a regenerator composed of 40% of  $\text{Gd}_{0.925}\text{Y}_{0.075}$  and 60% of Gd. This represented a 27.5%

performance increase compared to a single-layer regenerator. The improvement associated with a material with a lower  $T_C$  at larger temperature spans is due to a better use of its MCE at lower cold end temperatures.

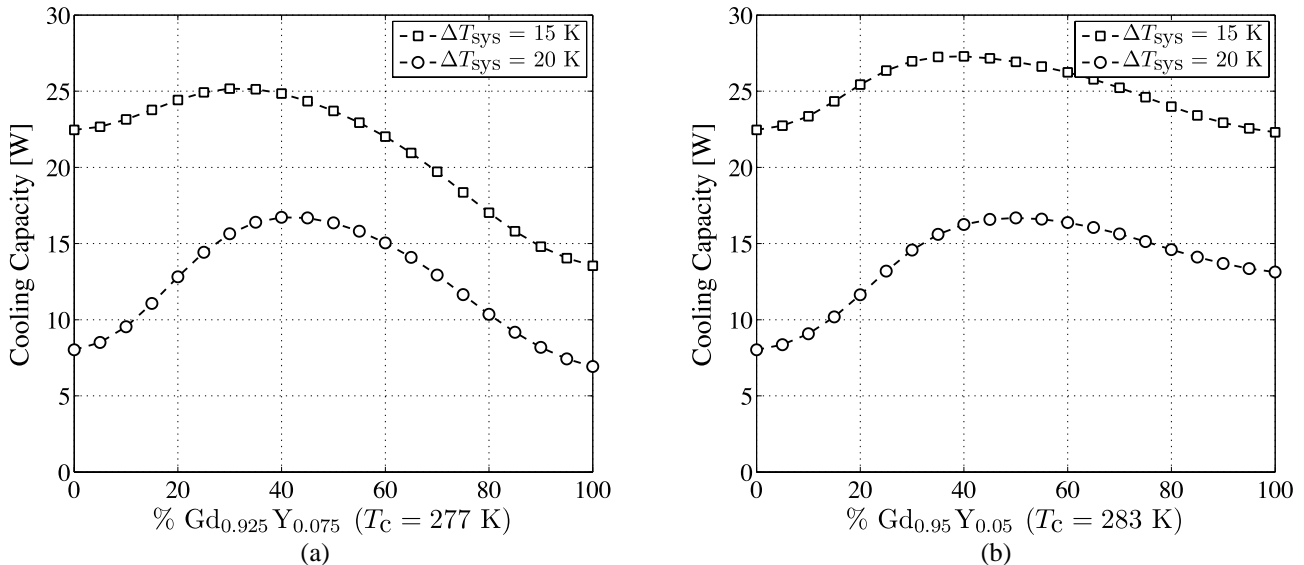


Figure 2. Cooling capacity as a function of the fraction of (a)  $Gd_{0.925}Y_{0.075}$  and (b)  $Gd_{0.95}Y_{0.05}$  in two-layer AMRs.

For the three-layered configuration of AMRs, the  $Gd_{0.975}Y_{0.025}$  was not used, since the configurations of a two-layer regenerator composed of  $Gd_{0.975}Y_{0.025}$  and Gd returned the lowest values for the cooling capacities. Thus, only one configuration of materials was used for the simulations of a three-layer regenerator, where different fractions of Gd at the hot end of the regenerator, fractions of  $Gd_{0.925}Y_{0.075}$  at the cold end of the regenerator and  $Gd_{0.95}Y_{0.05}$  in between were assumed. Gd was varied in steps of 10%, while the  $Gd_{1-x}Y_x$  alloys were varied in steps of 5%. The cooling capacity as a function of the different combination of length fractions in the three-layered regenerator for system temperature spans of 15 and 20 K are shown in Figs. 3(a) and 3(b), respectively. Here, the edge lines (for 0 and 100% fraction of each MCM) of the triangle in each figure represent the cases of two-layer AMRs, while the vertices correspond to the single layer AMRs. It can be seen in Fig. 3 that the performance of a three-layered regenerator with these MCM is always better than a two-layered regenerator as the cooling capacity increases from the edges to the inner part.

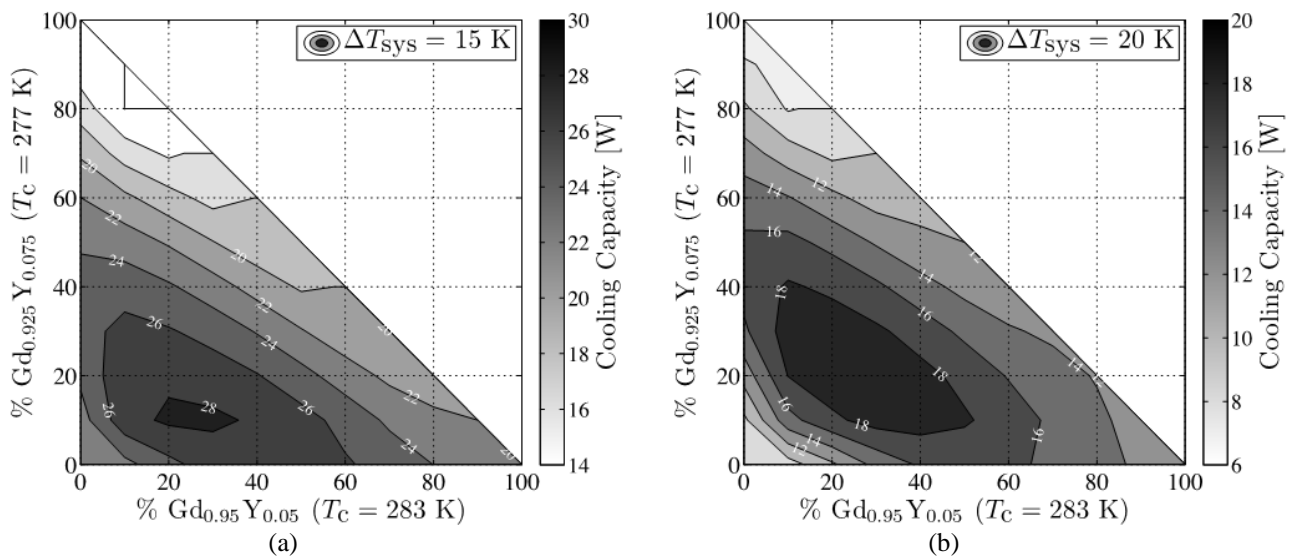


Figure 3. Cooling capacity as a function of the fraction of  $Gd_{0.925}Y_{0.075}$ ,  $Gd_{0.95}Y_{0.05}$  and Gd in three-layer AMRs for system temperature spans of (a) 15 K and (b) 20 K.

The maximum cooling capacity for a temperature span of 15 K (28.4 W) was obtained with a three-layer regenerator with 10%  $Gd_{0.925}Y_{0.075}$ , 30%  $Gd_{0.95}Y_{0.05}$  and 60% Gd. This corresponds to a performance improvement of 15.0% and 4.0%, in comparison with a single-layer and a two-layer regenerator, respectively. For a temperature span of 20 K, the

maximum cooling capacity (19.3 W) was attained with a three-layer regenerator with 20%  $Gd_{0.925}Y_{0.075}$ , 30%  $Gd_{0.95}Y_{0.05}$  and 50% Gd. This corresponded to a 47.3% increase in performance compared to a single-layer regenerator, and a 15.5 % increase in performance compared to a two-layer regenerator.

Four-layered AMR were simulated by varying the fraction of each of the four MCM in steps of 5%. The position of the materials in the regenerator was organized in ascending order of the Curie temperature, where the material with the lowest  $T_C$  (277 K) was allocated in the cold end of the regenerator, and the material with the highest  $T_C$  (290 K) was allocated in the hot end of the regenerator. Figure 4 shows the cooling capacity as a function of the different combinations of length fractions in the four-layered regenerator. Here, only the optimized configuration for each system temperature span is presented, where Fig. 4(a) is for a system temperature span of 15 K (60% of Gd in the regenerator), and Fig. 4(b) is for a system temperature span of 20 K (50% of Gd in the regenerator).

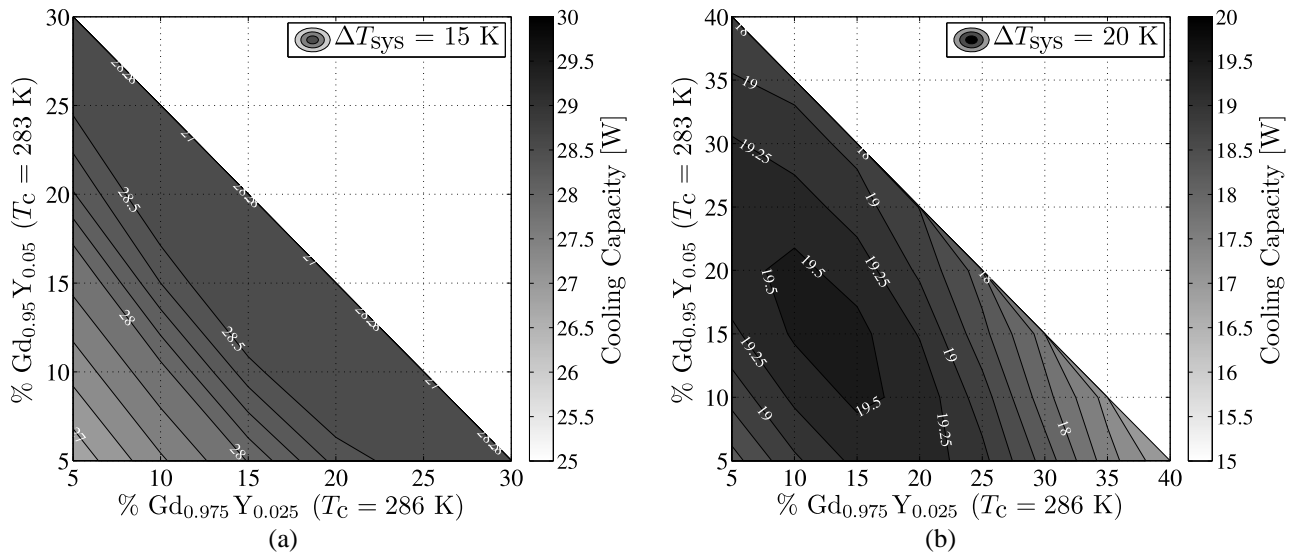


Figure 4. Cooling capacity as a function of the fraction of each of the four MCM in the optimized configurations for four-layer AMRs for system temperature spans of (a) 15 K (60% Gd) and (b) 20 K (50% Gd).

A maximum cooling capacity of 28.9 W for a temperature span of 15 K was obtained with a four-layer regenerator composed with 5%  $Gd_{0.925}Y_{0.075}$ , 20%  $Gd_{0.95}Y_{0.05}$ , 15%  $Gd_{0.975}Y_{0.025}$  and 60% Gd. This corresponds to a performance improvement of 17.0%, 5.9% and 1.8%, in comparison with a single-layer, two-layer and a three-layer regenerator, respectively. For a temperature span of 20 K, the maximum cooling capacity (19.6 W) was attained with a four-layer regenerator composed with 20%  $Gd_{0.925}Y_{0.075}$ , 15%  $Gd_{0.95}Y_{0.05}$ , 15%  $Gd_{0.975}Y_{0.025}$  and 50% Gd. This corresponded to a 49.6% increase in performance compared to a single-layer regenerator, 17.4% increase compared to a two-layer regenerator and a 1.5% increase compared to a three-layer regenerator. It can be seen that the increase in performance becomes less significant as the number of layers increase. For the operating conditions and Curie temperatures used in the simulations, the increase in performance achieved by using a four-layered AMR is minimal (only 1.5% for a system temperature span of 20 K) compared to a three-layered regenerator.

It is also worth noting that for both operating conditions, when a regenerator with two, three or four layers is considered, a high fraction (at least 50%) of Gd is necessary in order to achieve the highest cooling capacities. Further studies are already being carried out to determine the reason why those configurations of materials achieved the largest cooling capacities.

## 5. CONCLUSIONS

The performance of multilayer AMRs composed of Gd and three  $Gd_{1-x}Y_x$  alloys was evaluated in this work. A numerical model was used to evaluate the configuration of materials that resulted in the largest cooling capacity for a given operating point and a fixed temperature span. Results indicated that by increasing the number of layers, the cooling capacity also increases, especially for larger temperature spans. Working with a system temperature span of 15 K, the optimized configuration of a four-layer regenerator presented a 17.0% increase in performance compared to a single-layer regenerator. For a temperature span of 20 K, the performance was approximately 49.6% higher than that of a single-layer regenerator. However, for the operating conditions and Curie temperatures used in this work, the improvement in performance achieved by using a four-layer regenerator compared to a three-layer regenerator is

minimal (1.5% for a system temperature span of 20 K). Considering again the simulation parameters and MCMs used in this work, it can be concluded that at least 50% of Gd is necessary in the multilayer regenerator in order to achieve the largest cooling capacities. The optimized multilayer AMR will be experimentally tested in the test apparatus developed by Arnold *et al.* (2014).

## 6. ACKNOWLEDGEMENTS

The authors would like to acknowledge CNPq, Embraco and the EMBRAPPII Unit Polo/UFSC for financial support.

## 7. REFERENCES

- Arnold, D.S., Tura, A., Ruebsaat-Trott, A. and Rowe A., 2014. "Design improvements of a permanent magnet active magnetic refrigerator", *International Journal of Refrigeration*, Vol. 37, pp. 99-105.
- Eriksen, D., Engelbrecht, K., Bahl, C.R.H., Bjork, R., Nielsen, K.K., Insinga, A.R. and Pryds, N., 2015. "Design and experimental tests of a rotary active magnetic regenerator prototype", *International Journal of Refrigeration*, Vol. 58, pp. 14-21.
- Jacobs, S., Auringer, J., Boeder, A., Chell, J., Komorowski, L., Leonard, J., Russek, S. and Zimm, C., 2014. "The performance of a large-scale rotary magnetic refrigerator", *International Journal of Refrigeration*, Vol. 37, pp. 84-91.
- Kamran, M., Ali, H., Farhan, M., Tang, Y.B., Chen, Y.G. and Wang, H.S., 2016. "Performance optimization of room temperature magnetic refrigerator with layered/multi-material microchannel regenerators", *International Journal of Refrigeration*, In press.
- Nielsen, K.K., Bahl, C.R.H., Engelbrecht, K., Smith, A., Pryds, N. and Hattel, J., 2010. "Numerical modeling of graded active magnetic regenerators", *International Conference on Magnetic Refrigeration at Room Temperature*.
- Teyber, R., Trevizoli, P.V., Christiaanse, T.V., Govindappa, P., Niknia I. and Rowe A., 2016. "Performance evaluation of two-layer active magnetic regenerators with different second-order magnetocaloric materials". Submitted to *Applied Thermal Engineering*.
- Trevizoli, P.V., 2015. *Development of Thermal Regenerators for Magnetic Cooling Applications*. Ph.D. thesis, Federal University of Santa Catarina, Florianópolis, SC, Brazil.
- You, Y., Yu, S., Tian, Y., Luo, X. and Huang, S., 2016. "A numerical study on the unsteady heat transfer in active regenerator with multi-layer refrigerants of rotary magnetic refrigerator near room temperature", *International Journal of Refrigeration*, Vol. 65, pp. 238-249.

## 8. RESPONSIBILITY NOTICE

The authors are the only responsible for the printed material included in this paper.